

Thermoelectric Properties of Nanocrystalline Lead Telluride

Vikash Sharma^{1, a)}, Monika Saxena¹ and Gunadhor S. Okram¹

¹UGC-DAE Consortium for Scientific Research, Khandwa Road, University Campus Indore-452001, MP, India

^{a)}Corresponding author: vikashphy1@gmail.com

Abstract. Nanocrystalline (NC) lead telluride (PbTe) was successfully synthesized by polyol method and characterized thoroughly using various techniques. Much more significant impurity phase of Te was found in PbTe for preparation at ~ 180 °C than that prepared at 235 °C. With enhanced electrical resistivity $\rho \sim 6.8 \times 10^{-3} \Omega\text{-m}$, Seebeck coefficient $S \sim 445 \mu\text{V/K}$ and power factor $S^2/\rho \sim 29 \mu\text{W/m-K}^2$ at 300 K compared to those of bulk, they reveal semiconducting nature and holes as majority charge carriers of NC PbTe. They are attributed to quantum confinement effect, enhanced grain boundaries (GBs) and other crystal defects.

INTRODUCTION

Thermoelectric (TE) materials are gaining attention in research due to their many potential applications such as temperature measurements, waste heat recovery, air conditioning and refrigeration [1]. They have many advantages as they are not environmentally harmful, components with no moving parts, rapid response time, small size and high reliability [1]. The performance of a TE material is evaluated from its TE figure of merit defined by $ZT = S^2T/\rho\kappa$, where S is the Seebeck coefficient, ρ is the electrical resistivity, κ is the thermal conductivity and T is the absolute temperature. However, the interdependence and coupling of S , ρ , and κ have made extremely difficult to achieve $ZT > 1$ in a simple material. After active research of few decades, in 1993, Hicks and Dresselhaus [2] predicted that quantum confinement of electrons and holes in low-dimensional materials could dramatically increase $ZT > 1$ by independently changing power factor (S^2/ρ).

Bulk PbTe a state-of-art TE material with $ZT \sim 1$ near about 600 – 700 K are reported to exhibit $ZT > 1$ it is its nanocomposites, alloys, super-lattices and solid solution via nano-inclusion [3, 4]. Recently, Zhang et al. reported $ZT \approx 1.83$ at 773 K in n-type PbTe-4% InSb composites [3]. Particularly, these nanostructured materials are solid solutions and band structure engineered material, which reduces κ and enhances S^2/ρ simultaneously, making them change independently. However, synthesis of nanostructured materials using chemical method provides an easier way to tune their size, size distribution and shape using reaction time, temperature and combination of surfactants [5]. There are many chemical methods for synthesis of nanostructured materials reported such as thermal decomposition [6], polyol [7], ultrasound-assisted [8] and others [9]. We synthesized NC PbTe using low cost and easy one among other chemical methods called polyol method and studied its TE properties.

EXPERIMENTAL

Lead chloride, PbCl_2 (99.999%, Alfa Aesar), potassium tellurite monohydrate, $\text{K}_2\text{O}_3\text{Te.H}_2\text{O}$ (> 90%, Alfa Aesar) and diethylene glycol (DEG) (98.5%, Merck) were used as received for preparation of NC PbTe. Typically, 3 mmol each of PbCl_2 and $\text{K}_2\text{O}_3\text{Te.H}_2\text{O}$, and 30 ml DEG were mixed in three-neck round-bottom flask and heated it at the rate of 15 °C/min to ~ 180 °C. The mixture turned blackish at around 140 °C, indicating the initiation of decomposition of precursors and maintained the temperature at ~ 180 °C for 2 hours to complete the reaction. The reaction product was then cooled down to room temperature. Ethanol was added to dilute the product and centrifuged it at 12,000 rpm for 10 min. The resultant supernatant was discarded after retaining the black NPs. This step was repeated again to remove the excess DEG, if any. The precipitate was then vacuum-dried at 60 °C for 2 hours and used directly for further characterizations. This sample was denoted as PbTe1. With other conditions remaining the same, another sample PbTe2 was prepared at ~ 235 °C.

The Bruker D8 Advance x-ray diffractometer with Cu K_α of wavelength, 1.54 Å for x-ray diffraction (XRD) and LabRAM HR Visible instrument equipped with an Ar ion laser with a wavelength of 473 nm for Raman

spectroscopic measurements were used. For morphological studies, an atomic force microscope (AFM)nanoscope E, and digital instruments with a silicon nitride cantilever was employed to probe different portions of the cold-press pellet surface in contact AFM mode. Compositional determination was determined from energy-dispersive x-ray spectroscopy (EDAX) measurement using F Model JEOL JSM 5600.

RESULTS AND DISCUSSION

Fig. 1 (a) shows the XRD patterns of PbTe1 and PbTe2. PbTe1 has mixed phase of PbTe and Te perhaps near to equal proportion. However, XRD peaks of PbTe2 around $2\theta = 23.84^\circ, 27.70^\circ, 39.45^\circ, 46.60^\circ, 48.85^\circ, 57.03^\circ, 64.54^\circ, 71.50^\circ$ and 84.93° due to (111), (200), (220), (311), (222), (400), (420), (422) and (440) reflection planes, respectively, can be indexed and well-matched with face centered cubic (fcc) phase of PbTe (JCPDS# 01-077-0246) with some very feeble extra peaks (*), which are due to presence of Te. The lattice parameter $a = 6.4621$ of PbTe2 was found from Rietveld refinement analysis (Fig. 1 (b)). These results indicate that fccPbTe phase is the majority phase in PbTe2 with Teimpurity phase but with very significantly reduced proportion compared to that in PbTe1. The average particle size of PbTe2 calculated from Debye-Scherrer relation was found to be 51.4 ± 0.8 nm. Therefore, this study clearly shows that the secondary phase of Te in PbTeis reduced significantly with increase in reaction temperature from 180°C to 235°C .

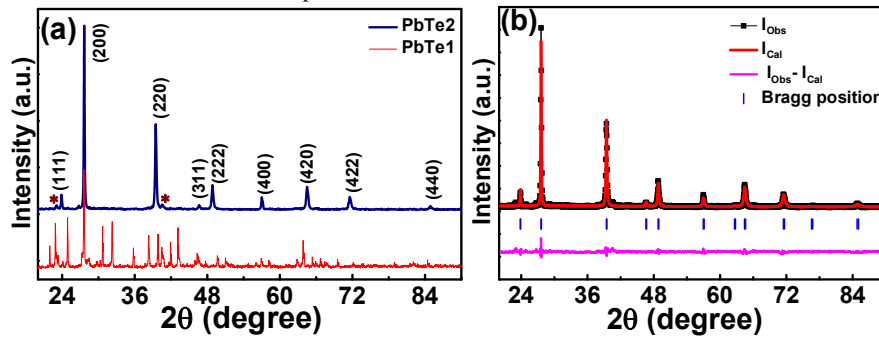


Fig. 1 (a) X-ray diffraction patterns of PbTe1 and PbTe2; starred (*) peaks are related to Te phase, and (b) Rietveld refinement of XRD data of PbTe2.

The 3D AFM micrograph of the compressed pellet of PbTe2 shows roundish, random shapes and different sizes of NCs (fig. 2(a)). The average particle size is found to be around 120 ± 20 nm, more than double that found from Scherrer relation. This difference is due to difference in detection technique as expected. The atomic percentage of Pb and Te in PbTe2 from EDAX data (fig. 2 (b)) are found to be Pb: Te = 48.75: 51.25 is a little deviated from that 1:1 expected in PbTe. This means that presence of extra Te is confirmed that found in XRD pattern. Considering that Pb present is fully utilized for making PbTe, atomic % of Te present is 2.5, which is relatively significant and hence might reflect in the electrical transport properties.

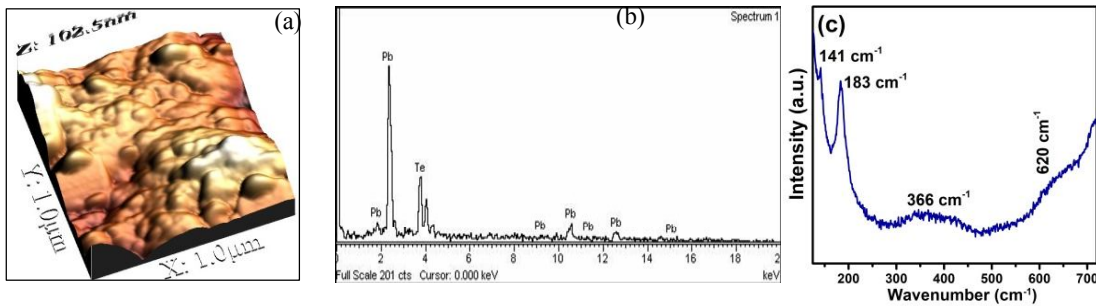


Fig. 2 (a) Atomic force microscopy image, (b) energy dispersive x-ray spectrum and (c) Raman spectra of PbTe2.

The vibrational modes in PbTe2 were determined using Raman spectra (fig. 2 (c)) that have four vibrational modes near at $141, 183, 366$ and 620 cm^{-1} , consistent with earlier report [10]. The mode appeared at 141 cm^{-1} comes from formation of TeO_2 due to laser induced local heating of the sample, which may be because of extra Te presence as found from EDAX data. A mode near at 183 cm^{-1} (w_0) with strong intensity is a coupled plasma-phonon mode of PbTe, and a broad hump like feature around 366 cm^{-1} is the $2w_0$ phonon mode [10]. Moreover, a mode around 620 cm^{-1} is a $4(\text{TO} + \text{LO})$ phonon mode in PbTe, where TO and LO means transverse and longitudinal optical mode, respectively [10].

ELECTRICAL TRANSPORT STUDY

Fig. 3 displays T-dependence on ρ , S and S^2/ρ of PbTe₂ sample. The cooling and warming cycle data of pure nearly identical (fig. 3 (a)). It decreases with increase in T and attained the value $6.8 \times 10^{-3} \Omega\text{-m}$ at 300 K, which indicates its semiconducting nature in T range 8 to 300 K. S, on the other hand, increases with increase in T and attains the maximum value of $445 \mu\text{V/K}$ at 300 K. Such trends in ρ and S are attributed to the mixed phase nature and NC nature of this sample and expected to be useful for TE properties or the power factor. Positive values of S over T range 90 to 300 K prove its p-type semiconducting nature.

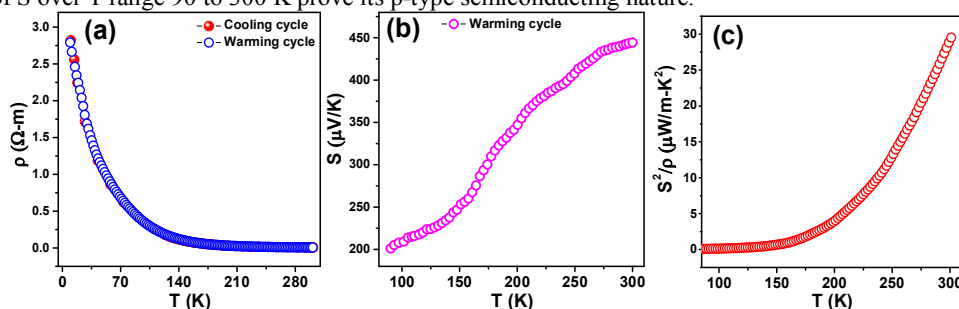


Figure 3 temperature dependent (a) electrical resistivity, (b) Seebeck coefficient and (c) power factor of PbTe₂.

As expected from ρ and S, power factor S^2/ρ also increases with T and attained a value $\sim 29 \mu\text{W/m-K}^2$ at 300 K. We found significantly enhanced S, ρ and S^2/ρ of $62 \mu\text{V/K}$, $25 \times 10^{-5} \Omega\text{-m}$ and $15 \mu\text{W/m-K}^2$, respectively, compared to those of bulk PbTe reported [11]. Since ZT is normally reduced in nanostructured materials compared to bulk, enhanced ZT of this NC PbTe is expected to be larger than that of bulk PbTe. This might be related to quantum confinement effects, enhanced scattering of charge carriers from GBs and change in band structures.

CONCLUSION

NC PbTe was successfully synthesized using a simple polyol method. The electrical transport properties reveal its p-type semiconducting nature. Electrical resistivity, thermopower and power factor found $\sim 6.8 \times 10^{-3} \Omega\text{-m}$, $\sim 445 \mu\text{V/K}$ and $\sim 29 \mu\text{W/m-K}^2$, respectively, at 300 K are larger than those reported in the bulk. It is attributed to various modified transport phenomena and change in band structures in this nanostructure.

ACKNOWLEDGEMENTS

Authors are thanked to Dr. M. Gupta/Mr. L. Bhera, Dr. D. M. Phase/ Mr. V. Ahire, Dr. V. Sathe/ Mr. A. Rathore, and Dr. V. Ganesan/ Mr. M. Gangarade, UGC-DAE Consortium for Scientific Research, Indore, India, for collecting XRD, EDAX, Raman data and AFM image, respectively.

REFERENCES

1. S. W. Finefrock, G. Zhang, J. H. Bahk, H. Fang, H. Yang, A. Shakouri and Y. Wu, *Nano Lett.* **14**, 3466–3473 (2014).
2. Y. M. Lin and S. Dresselhaus, *Phys. Rev. B - Condens. Matter Mater. Phys.* **68**, 1–14 (2003).
3. J. Zhang, D. Wu, D. He, D. Feng, M. Yin, X. Qin and J. He, *Adv. Mater.* **29**, 1–7 (2017).
4. T. C. Harman, P. J. Taylor, M. P. Walsh and B. E. LaForge, *Science* **297**, 2229–2232 (2002).
5. Tarachand, V. Sharma, R. Bhatt, V. Ganesan and G. S. Okram, *Nano Res.* **9**, 3291–3304 (2016).
6. V. Sharma, C. Chotia, Tarachand, V. Ganesan and G. S. Okram, *Phys. Chem. Chem. Phys.* **19**, 14096–14106 (2017).
7. V. Sharma, Tarachand, V. Ganesan and G. S. Okram, *AIP Conf. Proc.* **1731**, 1–4 (2016).
8. D. Verma, V. Sharma, G. S. Okram and S. Jain, *Green Chem.* **19**, 5885–5899 (2017).
9. V. Sharma, Tarachand, C. Chotia and G. S. Okram, *AIP Conf. Proc.* **1832**, 050085-1–050085-3 (2017).
10. B. Zhang, C. Cai, H. Zhu, F. Wu, Z. Ye, Y. Chen, R. Li, W. Kong and H. Wu, *Appl. Phys. Lett.* **104**, 161601 (2014).
11. Y. Pei, X. Shi, A. LaLonde, H. Wang, L. Chen and G. J. Snyder, *Nature* **473**, 66–69, (2011).